Journal of Nuclear Materials 403 (2010) 198–203

Contents lists available at ScienceDirect

Journal of Nuclear Materials

journal homepage: www.elsevier.com/locate/jnucmat

Effects of mechanical alloying on characteristics of nanocrystalline Fe–Cr–W–Ti–Y_2O_3 powders

Zhenhua Yao, Weihao Xiong *, Ming Yuan, Qianyun Peng

State Key Laboratory of Material Processing and Die & Mould Technology, Hua Zhong University of Technology, Wuhan 430074, China

ARTICLE INFO

Article history:
Received 2 August 2009
Accepted 16 June 2010

ABSTRACT

Effects of mechanical alloying (MA) parameters on characteristics of nanocrystalline Fe–Cr–W–Ti–Y_2O_3 powders, including alloying degree, grain size, microhardness and morphology had been systematically investigated by X-ray diffraction (XRD) and scanning electron microscopy (SEM). The results showed that the alloying degree of milled powders was increased with the elevation of milling rotational speed and elongation of milling duration. The W atoms were completely dissolved into the iron matrix after milling at 350 rpm for 24 h. The grain size of milled powders was decreased sharply at first stage of milling and leveled off after 24 h, while lattice strain was increased. The microhardness of alloyed powders was elevated firstly and stabilized at about 607.4 HV after 24 h milling. Process control agent (PCA) effected the morphologies and retarded the alloying extent of the milled powders. Finer, more uniform and spherical particles were obtained when steric acid (SA) was chosen as PCA. Increasing ball to powder ratio (BPR) would lead to efficient reduction of average particle size, but decrease powder yield and increase contamination.

1. Introduction

Recently progresses were found in the researches of nanostructure ferrite alloy (NFA) with nominal composition Fe–(12–14)Cr–W–Ti–Y_2O_3 [1–5], which was potentially used as structure material in future fusion system due to their outstanding resistance to high temperature creep and irradiation [6–8]. Such alloys generally contain complex Y–Ti–O nanoclusters, which are derived from Y, O and Ti atoms dissolved in the matrix by MA [9,10].

Researchers have been conducted in order to control the size and distribution of oxide particle in the matrix of NFA by modifying chemical compositions [11–15]. Warm consolidation procedures following MA and annealing such as vacuum sintering, hot extrusion (HE) and hot isostatic pressing (HIP) have also been concentrated onto optimize the final microstructure and properties of this material [1,9,16]. The effects of these consolidation procedures on materials were sensitive to the characters of the starting powders, including morphology, grain size and contamination, etc. [17–19]. So the macroscopic properties of materials were related to the characters of starting powders severely.

However, there was no quantified understanding about the characters of powders with nominal composition Fe–(12–14)Cr–W–Ti–Y_2O_3 fabricated by MA. So in this work, the relations between parameters of milling and characteristics of powders were systematically studied.

2. Materials and methods

The iron powder had a purity of more than 99.5 wt.%, with a average particle size of 6 μm, while corresponding values for chromium, tungsten, titanium and yttrium oxide powder used were 99.95, 99, 99, 99.5 wt.% and 75 μm, 60 μm, 54 μm, 50 nm, respectively. Both vials and balls were stainless steel. Two sizes of balls (6 mm, 10 mm) with the total mass of 600 g were used in each vial, and the mass ratio of the two sizes of balls was 3:1. Ar_2 with 99.99% purity was filled in the vials to avoid oxidation of powders during MA.

Elemental powders with the nominal composition Fe–12Cr–2.5 W–0.4Ti–0.3Y_2O_3 in wt.% were mechanically alloyed in an attrition-type ball mill with parameters stated in Table 1. The effects of rotational speed, milling duration, PCAs, and BPR on characteristics of milled powders, including alloying extent, morphology, microhardness, etc. were investigated respectively by the comparison of (A, B, C), (C, D, E, F, G), (C, H, I, J, K, L) and (M, G, N, O). SA, alcohol and n-heptane were used as PCA.

The effects of milling duration and PCAs on alloying extent of powders were analyzed using X'PertPRO X-ray diffraction with Cu Kα, and the grain size and lattice distortion were estimated as Scherrer's equation [20]. Parts of powders milled for different duration were inlayed with mixture of epoxy and ethylenediamine, subsequently were grinded and polished, then microhardness of these powders were measured on HXS–1000AK microhardness tester. Five points were collected for each sample to make sure the accuracy. The effects of milling duration, PCAs and BPR on

* Corresponding author. Tel./fax: +86 027 87556247.
E-mail address: whxiong@mail.hust.edu.cn (W. Xiong).

0022-3115/$ - see front matter © 2010 Elsevier B.V. All rights reserved.
doi:10.1016/j.jnucmat.2010.06.027

Table 1
Parameters of MA.

Number	Rotational speed (r/min)	Milling duration (h)	PCA	BPR
A	220	48	No	20:1
B	280	48	No	20:1
C	350	48	No	20:1
D	350	0	No	–
E	350	6	No	20:1
F	350	12	No	20:1
G	350	24	No	20:1
H	350	48	0.5 wt.% SA	20:1
I	350	48	1 wt.% SA	20:1
J	350	48	2 wt.% SA	20:1
K	350	48	5 vol.% alcohol	20:1
L	350	48	5 vol.% n-heptane	20:1
M	350	24	No	15:1
N	350	24	No	25:1
O	350	24	No	30:1

morphology of powders were observed by Quanta-200 scanning electronic microscope.

Powder yield describes actual amount of alloyed powders obtained by MA. It was estimated as the ratio of the actual mass of powders obtained by MA with the mass of powders filled in vials. Contamination during MA was estimated by the following equation:

$$\eta = \frac{M_1 - M_2}{M_1} \quad (1)$$

where η represents the contamination, M_1 represents the weight of balls filling in the vial, and M_2 represents the weight of balls after MA, which has been cleaned and dried before weighing.

3. Results

3.1. Milling duration and milling rotational speed

Shown in Fig. 1 is the XRD patterns of milled Fe-based alloyed powders with different milling rotational speed (A–C) and milling duration (C, E–G). The XRD pattern of the powders mixture without milling (D) was present for comparison. It can be seen from pattern (D) that reflection peaks of Ti and Y_2O_3 were hardly ascertainable even in the curve corresponding to the powders without milling. Besides the position of reflection peaks of Fe and Cr were nearly coincident with each other. Comparison of (A–D) showed that the reflection peak of W in the powders milled for 48 h existed until the rotational speed reached 350 r/min. Curves of (C, E–G) exhibited reflection peak of W disappeared after 24 h milling under 350 r/min, and the position of α-(Fe, Cr) reflection peak shifted to lower angle with the milling.

Based on full width at half maximum (FWHM) of α-(Fe, Cr) reflections and Scherrer's equation, the grain size and lattice distortion of milled powders were estimated and presented in Fig. 2. The grain size was decreased rapidly at early stage of milling and leveled off at prolonged milling duration, while the lattice distortion was increased. Fig. 3 shows that the microhardness of milled powders was elevated sharply and stabilized at about 607.4 HV after 24 h milling.

SEM images of powders with different milling duration, corresponding to (D, E, F, G, C) in Table 1, were presented in Fig. 4. Severe agglomeration and formation of laminar structure were observed at first stage of milling (Fig. 4b), and the particle size ranged approximately from 10 μm to 100 μm. After milling for 48 h, equiaxed particles with size of less than 10 μm were found.

3.2. PCAs

Shown in Fig. 5 were XRD patterns of milled powder with PCAs varying in type and content. By comparison of (C), reflection peaks of W had not disappeared in all (H–L) patterns, but the strength of the peak was weakened with the decrease of SA addition.

Fig. 6 shows the morphologies of powders milled with and without PCAs. Finer, more uniform and spherical powders were obtained when SA was added into the milling. The particles were mostly less than 5 μm when the amount of SA reached 2 wt.%. Laminar powders were obtained when alcohol was added, and the morphology of powders were insensitive to addition of n-heptane by comparison of Fig. 6e and f.

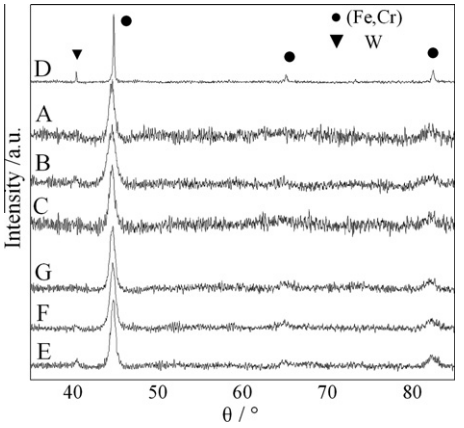

Fig. 1. XRD patterns of milled Fe-based alloy with different rotational speed and milling duration.

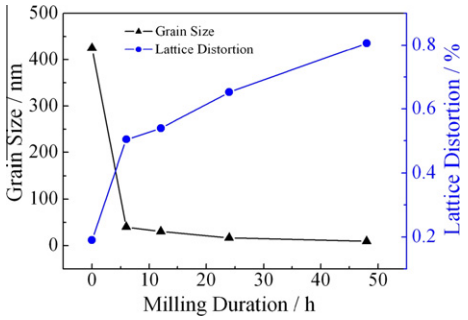

Fig. 2. Grain size and lattice distortion of milled Fe-based alloy as a function of milling duration.

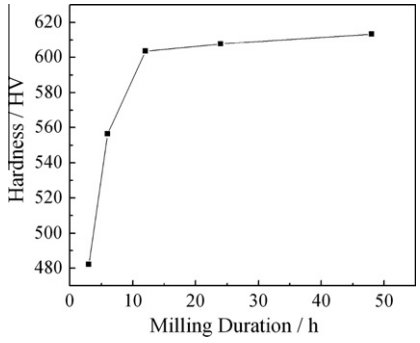

Fig. 3. Hardness of milled powder as a function of milling duration.

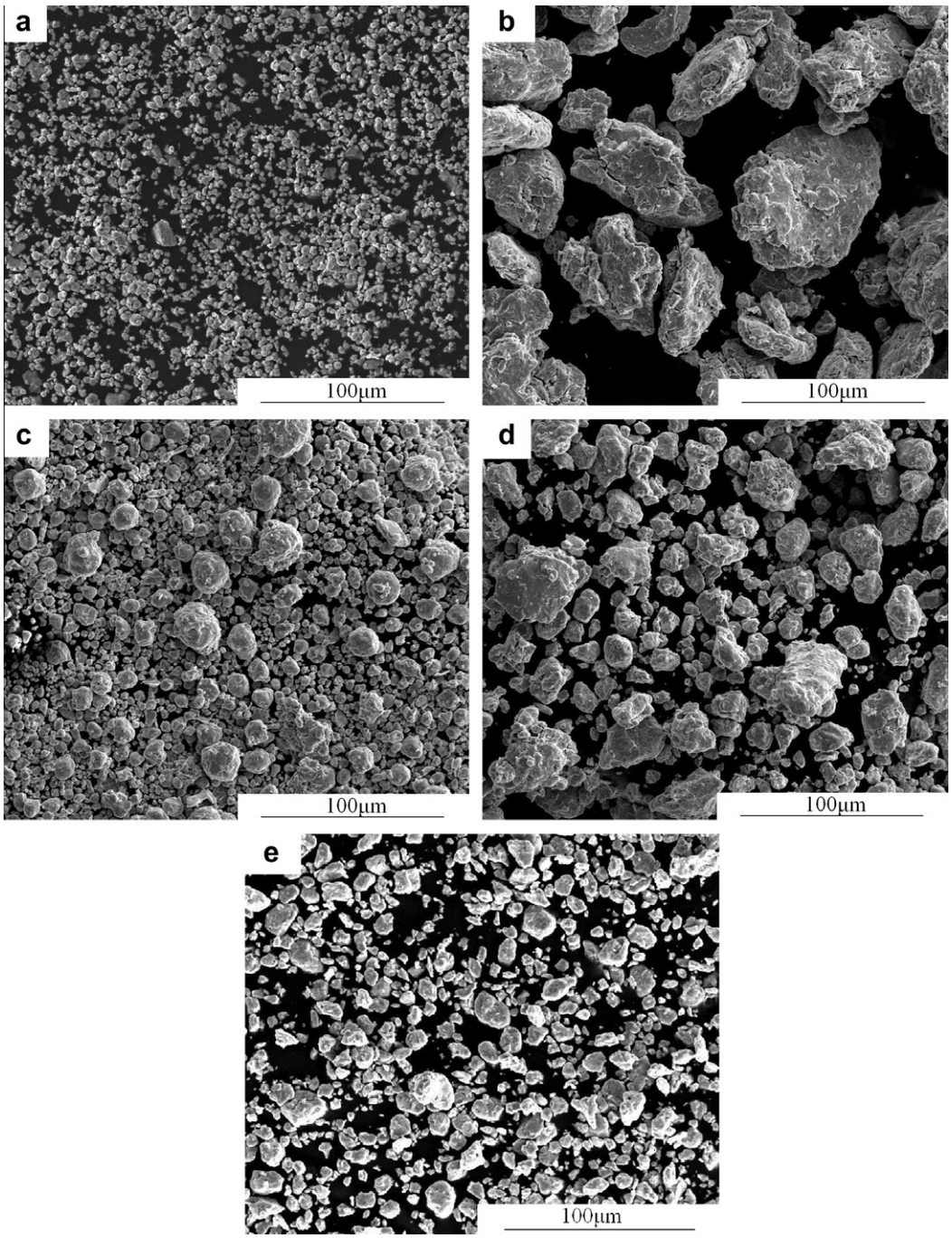

Fig. 4. SEM images of powders milled with different duration: (a) powder D, 0 h; (b) powder E, 6 h; (c) powder F, 12 h; (d) powder G, 24 h; (e) powder C, 48 h.

3.3. BPR

Fig. 7 shows the SEM graphs of powders milled for 24 h with different BPR. The average particle size was decreased with elevation of BPR. However, excessively high BPR, which increased the times of collision of balls on powders, would cause undesirable contamination and low powder yield, as seen in Fig. 8.

4. Discussion

The decrease of strength of reflection peaks of W in Fig. 1 indicated that the alloying extent was enhanced with the elongation of milling duration and increase of milling rotation speed, which was consistent to the study by Suryanarayana [21]. It was easy to realize that faster mill rotational speed and longer milling duration would lead to higher energy inputted to powders. The change of position of reflection of α-(Fe, Cr) peak indicated the solution of W atoms and increase of strain distortion. The broadening of reflection of α-(Fe, Cr) peak indicated the decrease of average grain size of α-(Fe, Cr), which was shown in Fig. 2. It would be inferred that a balance have been established between deformation and recovery of the grains and W atoms have dissolved in the α-grain structure completely after 24 h milling because the change of average grain size and microhardness of milled powders were not obvious, which have been suggested by Y. Kimura et al. referred to

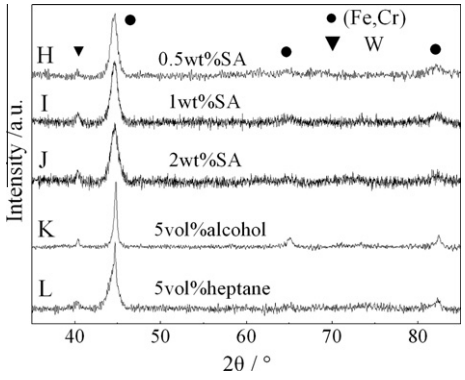

Fig. 5. XRD patterns of milled powders with PCAs.

alloyed Fe–24Cr–(0–15)Y_2O_3 powders fabricated by MA [15]. The morphologies of powders with different milling duration exhibited a typical process of milling for ductile particles [22]. At first stage of milling, powders could withstand the deformation and be welded together. With the continued milling, the powders were hardened and fractured to be small particles.

SA and alcohol have effectively prevented the agglomeration between powders, while no changes occurred when n-heptane was added. The PCAs was absorbed on the surfaces of the Fe-based powders as surface-active agents, therefore the surface tension of the solid material was lowered, which resulted in the reduce of surface energy, so the agglomeration of powders was inhibited, and the equilibrium between fracturing and cold welding was established till the particles was very fine. Meanwhile, the PCAs absorbed on the surface of powders could prevent the direct contact

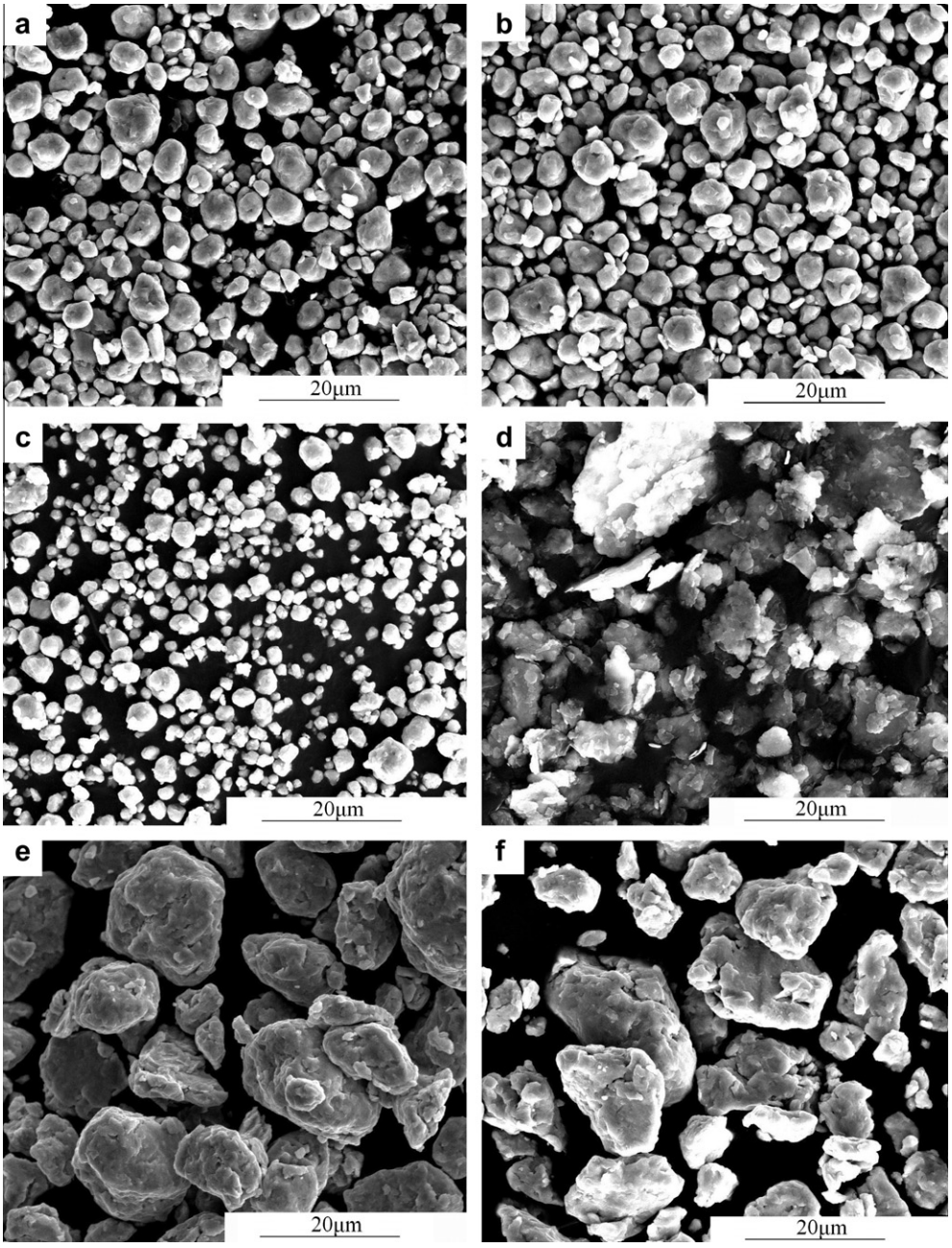

Fig. 6. SEM graphs of milled powder with PCAs: (a) powder H, 0.5 wt.% SA; (b) powder I, 1 wt.% SA; (c) powder J, 2 wt.% SA; (d) powder K, 5 vol.% alcohol; (e) powder L, 5 vol.% n-heptane; (f) powder C, no PCA.

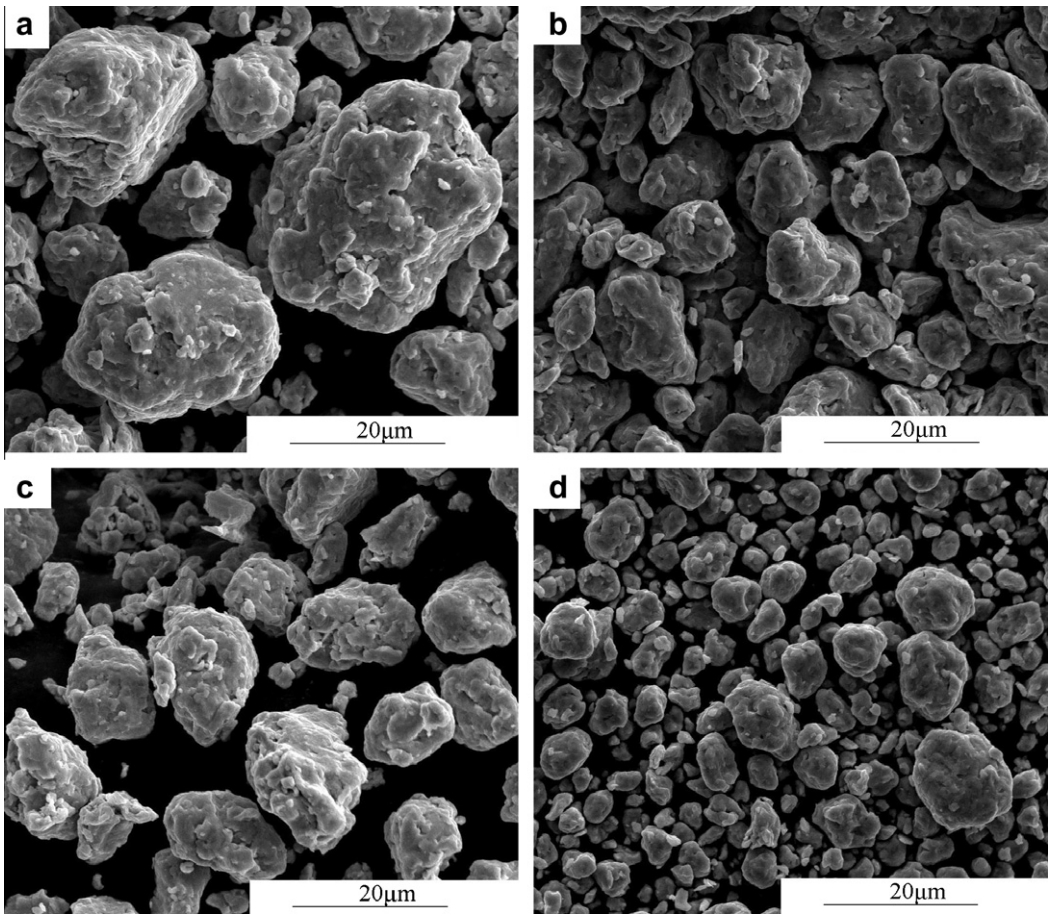

Fig. 7. SEM graphs of milled powder with different BPR: (a) powder M, 15:1; (b) powder G, 20:1; (c) powder N, 25:1; (d) powder O, 30:1.

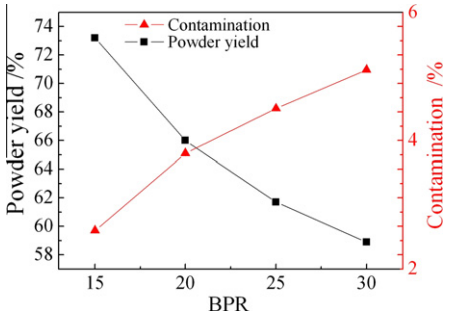

Fig. 8. Powder yield and contamination as a function of BPR.

between powders' surfaces, so the interdiffusion of atoms was hindered; therefore the alloying extent was decreased. The different impacts of PCAs on powders have not a clear explanation, however, L. Shaw et al. suggested that this difference was related to the physical properties such as melting point and phase transformation behavior [23].

Given the same milling rotational speed and milling duration, higher BPR would result in finer particles, because the collision per unit time was increased and more energy was transferred to powders, so the hardening of powders was accelerated and the equilibrium was established quickly. Meanwhile, high frequency of collision would lead to serious adhesion of powders to milling mediums, so more milled powder would left on the walls of vials and surface of balls. Thus the milled powders obtained actually were lessened, so the powder yield was decreased. Additionally, it was easy to understand that the contamination caused by collision, wear between milling mediums was increased with higher BPR.

5. Conclusions

Nanocrystalline powders with nominal composition Fe–Cr–W–Ti–Y_2O_3 have been synthesized by mechanical alloying, and the effects of parameters of MA on alloyed powders have been systematically studied. The following findings were obtained as a result:

(1) Elevation of milling speed and duration would increase the rate of alloying. The W atoms were completely dissolved into iron base after milling at 350 rpm for 24 h. The average size of α-(Fe, Cr) and microhardness of milled powders were stabilized at about 19 nm and 607.4 HV individually after 24 h milling.
(2) Addition of SA could effectual inhibit the agglomeration of milled powders. With increasing the SA addition, the milled powders were more spherical and uniform. When the addition of SA reached to 2 wt.%, the average particle size was less than 5 μm. However, the existence of PCAs would retard the rate of alloying.
(3) Increasing BPR would reduce average size of milled powders, but lead to lessened powder yield and increased contamination.

The implication of the present work was that the selection of parameters of MA should be intelligently judged, by which the

characters of powders could be controlled. For example, addition of SA would reduce the agglomeration, while excessive SA could retard the alloying rate, so the amount of SA addition used for this material should be properly judged. Thus the ideal powders for warm consolidation could be obtained efficiently, and the final properties of materials would be optimized.

Acknowledgements

This work was financially supported by Key Program of National Natural Science Foundation of China, NSFC 50634060. Supports provided by Analytical and testing center in Huazhong University of Science & Technology were also acknowledged.

References

[1] M.J. Alinger, G.R. Odette, D.T. Hoelzer, Acta. Mater. 57 (2009) 392–406.
[2] I.S. Kim, J.D. Hunn, N. Hashimoto, D.J. Larson, P.J. Maziasz, K. Miyahara, E.H. Lee, J. Nucl. Mater. 280 (2000).
[3] S. Ukai, A. Kohyama, A. Kimura, T. Hirose, K. Shiba, Report of IEA Workshop on Reduced-Activation Ferritic/Matensitic Steels, JAERI-Conf. 2001–2007, pp. 282.
[4] D.J. Larson, P.J. Maziasz, I.S. Kim, K. Miyahara, Scripta Mater. 44 (2001) 359–364.
[5] D.S. Gelles, J. Nucl. Mater. 233–237 (1996) 293.
[6] G.R. Odette, M.J. Alinger, B.D. Wirth, Annu. Rev. Mater. Res. 38 (2008) 471.
[7] R. Lindau, A. Moslang, M. Schirra, P. Schlossmacher, M. Klimenkov, J. Nucl. Mater. 307–311 (2002) 769–772.
[8] R.L. Klueh, D.S. Gelles, S. Jitsukawa, A. Kimura, G.R. Odette, B. van der Schaaf, M. Victoria, J. Nucl. Mater. 307–311 (2002) 455–465.
[9] S. Ukai, M. Fujisawa, J. Nucl. Mater. 307–311 (2002) 749.
[10] H. Kishmoto, M.J. Alinger, G.R. Odette, T. Yamamoto, J. Nucl. Mater. 329–333 (2004) 367–371.
[11] S. Ohtsuka, S. Ukai, M. Fujiwara, T. Kaito, T. Narita, J. Phys. Chem. Solids 66 (2005) 571–575.
[12] N. Mizutani, Y. Tajima, M. Kato, J. Am. Ceram. Soc. 59 (2006) 168–171.
[13] T. Okuda, S. Nomura, S. Shikakura, K. Asabe, S. Tanoue, M. Fujiwara, in: Proc. Symp. Sponsored by the TMS Powder Metallurgy Committee, Indiana, 1989, pp. 195.
[14] T. Okuda, M. Fujiwara, J. Mater. Sci. Lett. 14 (1995) 1600.
[15] Y. Kimura, S. Takaki, S. Suejima, R. Uemori, H. Tamehiro, ISIJ Int. 39 (1999) 176.
[16] P. Olier, A. Bougault, A. Alamo, Y. de Carlan, J. Nucl. Mater. 386–388 (2009) 561–563.
[17] Z. Hussain, C.G. Tan, B Projjal, Mater. Des. 31 (2010) 2211–2215.
[18] M. Azabou, M. Khitouni, A Kolsi, Mater. Charact. 60 (2009) 499–505.
[19] G. Gonzale, L. D'Angelo, J. Ochoa, D Bonyuet, Mater. Sci. Forum 386–388 (2002) 153–158.
[20] B.E. Warren, London, Addison-Wesley Pub Co., 1996, pp. 25.
[21] C. Suryanarayana, Prog. Mater. Sci. 46 (2001) 1–184.
[22] C. Suryanarayana, E. Ivanov, V.V. Boldyrev, Mater. Sci. Eng. 304–306 (2001) 151–158.
[23] L. Shaw, M. Zawrah, J. Villegas, H. Luo, D. Miracle, Mater. Sci. Eng. A 34A (2003) 159–170.